ChemComm

Accepted Manuscript

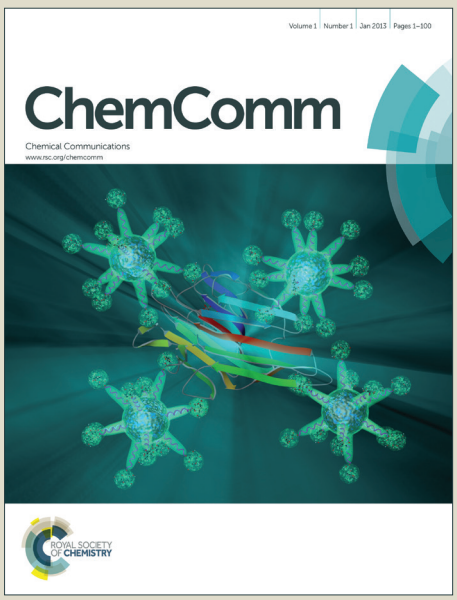

ROYAL SOCIETY OF CHEMISTRY

www.rsc.org/chemcomm

Journal Name

RSCPublishing

COMMUNICATION

Rational Design of an Orthosteric Regulator of hIAPP Aggregation

Cite this: DOI: 10.1039/x0xx00000x

De-Sheng Zhao[a], Yong-Xiang Chen[a], Yan-Mei Li*[a, b]

Received 00th January 2012,
Accepted 00th January 2012

DOI: 10.1039/x0xx00000x

www.rsc.org/

Developing compounds regulating amyloid toxic oligomers but not fibrils formation should constitute an effective strategy for the treatment of Diabetes. Based on the full understanding of the folding mechanism, we designed an orthosteric helix regulator that can promote hIAPP to assemble into large non-cytotoxic oligomers. As a result, the islet cells were protected.

Human islet amyloid polypeptide (hIAPP), also known as amylin, is a 37-residue peptide. It is produced by the β-cells along with insulin and plays an important role in controlling gastric emptying, glucose homeostasis, and suppression of glucagon release.[1] In 1987, hIAPP was found to be the primary component of the amyloid deposits around the β-cells in patients with Type 2 Diabetes. The formation of the islet amyloid can lead to β-cell dysfunction, death, and reduction in β-cell mass. [2] To prevent the β-cell from being harmed, inhibitors have been designed recently and found to markedly prevent the formation of islet amyloid fibrils.[3-10] However, a growing body of evidence has identified amyloid oligomers formed in the early stage as the basic cytotoxic components of the aggregation pathway[11-15] and most of these inhibitors have little effect on the formation of hIAPP toxic oligomers. Besides, oligopyridylamide α-helix mimetics have been designed as agonists and antagonists of hIAPP fibril formation.[16] However, whether the oligopyridylamide compound can regulate hIAPP oligomers formation kept unknown. Encouragingly, for β-amyloid and insulin, new inhibitors that target amyloid folding intermediate in the early stage have been successfully rationally designed.[17-19] Accordingly, the design of new inhibitors targeting the intermediates in the early stage and blocking the formation of toxic hIAPP oligomers should constitute an effective strategy for the treatment of Type 2 Diabetes.

Numerous investigations have suggested that amyloid oligomers are β-sheet–rich structures.[20, 21] Additionally, a β-strand-rich dimer has been included in the aggregation pathway as this structure appears to have the greatest likelihood of forming oligomers.[22, 23] Our converged replica exchange molecule dynamic (REMD) simulations suggested that the β-strand-rich dimers were formed through an α-helix-to-β-sheet transition mechanism (Fig. 1a). The hIAPP monomer may adopt a variety of conformations and it is very difficult for the hIAPP monomer to misfold into β-rich conformations directly, as the potential energy barrier is too high and the energy basins are very shallow (Fig. S4 in SI). Because the helix intermediates are the prerequisite and rate determining step in the formation of β-strand-rich dimers, which once formed, will rapidly and easily assemble into oligomers, we reasoned that artificial α-helices that mimic hIAPP could enhance the formation of helix intermediates and markedly promote hIAPP aggregation. By chaperoning IAPP through fusion to the maltose binding protein, the crystal structure of the hIAPP helix dimer has been obtained.[24] Computational analysis identified Leu12 and Phe15 as residues that contribute most strongly to the interaction of the hIAPP helix dimer (Fig. 1b). Thus, we designed a stable helix peptide which mimics the fragment $hIAPP_{12\text{-}15}$. To stabilize the short peptide in α-helical conformation, the hydrogen bond surrogate (HBS) approach has been adopted (Fig. 1d) in which the hydrogen bond between the carboxyl of i^{th} residues and the amide of $i+4^{th}$ residues is surrogated by carbon-carbon bonds. We chose HBS helices as they have shown high affinity and specificity previously when targeted to protein receptors.[25, 26]

We optimized the sequence using a sequence tolerance method.[27] L12 and F15 were proven to be the best choices to enhance the helix-helix interaction. It corresponds with the native peptide. We proposed to replace L16 with a glutamic acid to enhance the solubility and to stabilize the α-helical conformations (Fig. 1c). Further CD spectroscopy studies on control peptides (mutation of hot spot residues to alanine) showed that these residues are essential to stabilize the helical conformation (Fig. S7 in SI). Alanine was used as the backbone for its high helix-forming propensity. To further increase the contents of helix structures, the C-terminus was modified with N-methylamine. This resulted in the optimized sequence: ALAAFEA-NH-Me. For more information of the α-helix-to-β-sheet transition mechanism and peptide design strategy, see

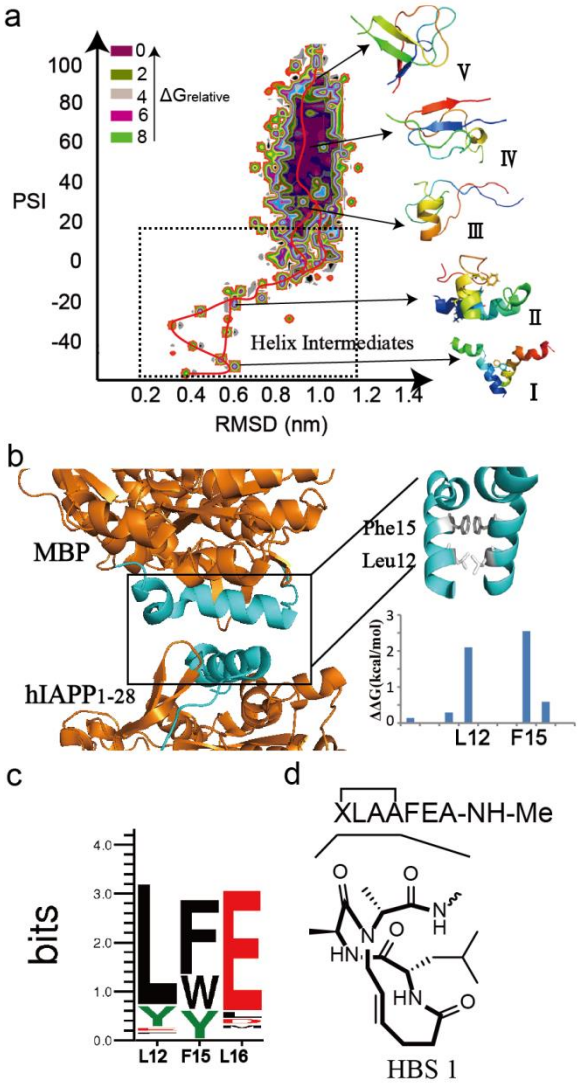

Figure 1. The helix-helix interaction of hIAPP dimer and rational design of the synthetic peptide. (a) Two-dimensional free energy maps for hIAPP7-29 dimer at 300 K as a function of average Psi angle of only one chain and the root mean square deviation (nm). Representative structures in each minimum-energy basin are also given: (I) (0.444, -41.75); (II) (0.46, -25.25); (III) (0.7425, 56.45); (IV) (0.80, 63.25); (V) (0.98, 109.15); the red line represents the conformation transition pathway. (b) Crystal structure of the maltose binding protein (MBP) - hIAPP fusion proteins (PDB code: 3G7V). Virtual alanine scanning suggests that hot spots of the helix dimer are L12 and F15 (inset). (c) The hIAPP helix-helix interface tolerance prediction. The optimized sequence was XLXXFEX (X represents any amino acid). (d)The hydrogen bond surrogate (HBS) helices structure. The intra-molecular hydrogen bond between i and i+4 residues has been replaced with a covalent carbon-carbon bond. The sequence of the optimized hIAPP mimetic HBS 1 is shown. *X* represents a 4-pentenoic acid residue. *Me* represents methyl.

Supplementary Results. The HBS helices were synthesized as previously reported [28-30] (Fig. S1 and Fig. S2 in SI).

The optimized HBS helix, HBS 1 (Fig. 1d), was judged to be 83% helical in 10% trifluoroethanol (TFE) in PBS and 67% helical in PBS only (Fig. S7 in SI). The high docking score and low docking RMSD values when HBS 1 was docked to hIAPP suggested that

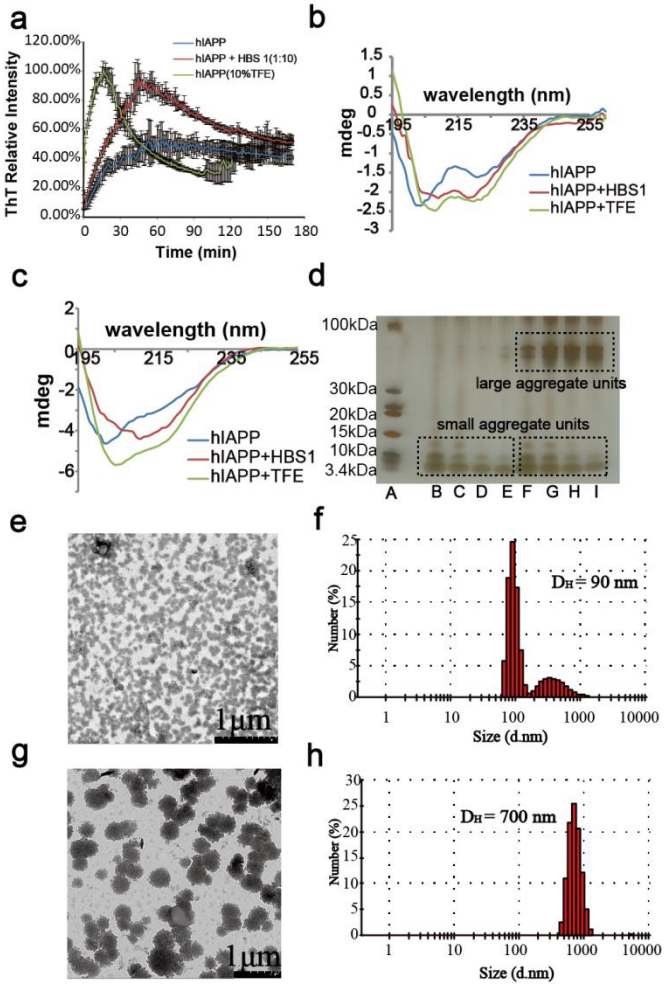

Figure 2. Effect of HBS 1 on hIAPP aggregation kinetic behaviors. (a) ThT fluorescence of hIAPP only (blue line, 10 μM), in the presence of HBS 1 (red line, 100 μM) and in the presence of 10% TFE (green line). (b) CD spectrum of hIAPP helix intermediates. Data was measured immediately after peptide dissolution. Blue line: hIAPP (10 μM); red line: hIAPP (10 μM) + HBS 1 (100 μM) Absorbance induced by HBS 1 was subtracted; green line: hIAPP (10 μM) in 10% TFE. (c) CD spectrum of hIAPP β-sheet conformation after incubation for 140 min. Blue line: hIAPP (10 μM); red line: hIAPP (10 μM) + HBS 1 (100 μM) Absorbance induced by HBS 1 was subtracted; green line: hIAPP (10 μM) in 10% TFE. (d) The peptide composition of hIAPP (30 μM) in the absence and presence of HBS 1 (300 μM) monitored by PICUP SDS-PAGE-silver staining. For lane (A): Marker; (B) hIAPP 30 μM, 20min; (C): hIAPP 30 μM, 80 min; (D): hIAPP 30 μM, 140 min; (E): hIAPP 30 μM, 200 min; (F): hIAPP 30 μM and HBS 1 300 μM, 20 min; (G): hIAPP 30 μM and HBS 1 300 μM, 80 min; (H): hIAPP 30 μM and HBS 1 300 μM, 140 min; (I): hIAPP 30 μM and HBS 1 300 μM, 200 min; (e) The TEM image of hIAPP small oligomers after incubation for 60 min. (hIAPP: 10 μM) (f) DLS analysis of small oligomers formed by hIAPP only after incubation for 60 min (hIAPP: 10 μM). (g) The TEM image of large globular oligomers in the presence of HBS 1 after incubation for 60 min. (hIAPP: 10 μM; HBS1: 100 μM). (h) DLS analysis of large globular oligomers formed by hIAPP in the presence of HBS 1 after incubation for 60 min. (hIAPP: 10 μM; HBS1: 100 μM).

HBS 1 can bind to hIAPP efficiently (Fig. S6 in SI). The free energy

surface of HBS 1 suggested that it could fold to the helix conformation with high probability (Fig. S8 in SI). When assayed in a Thioflavin T (ThT) fluorescence kinetic study, the designed compound promoted hIAPP aggregation (Fig. 2a). In the presence of HBS 1, hIAPP quickly assembled to an intermediate with a high ThT fluorescence signal. These intermediates then transformed slowly to another aggregation state with a decrease of ThT fluorescence intensity. Furthermore, 10% TFE was used as a positive control to induce amyloid aggregate through an α-helix aggregation mechanism.[31] We also found that in the presence of 10% TFE, hIAPP can assemble rapidly to an intermediate with high ThT fluorescence intensity and could then transfer to other aggregation states and attain a plateau (Fig. 2a). Circular Dichroism spectroscopy suggested that addition of HBS 1 or trifluoroethanol can promote hIAPP folding to helix-rich intermediates firstly (Fig. 2b), followed by conversion to β-rich structures (Fig. 2c). Besides, during the process of hIAPP aggregation, HBS 1 maintained its helix conformation and could not interact with ThT (Fig. S12 and S14c in SI). For more details about conformation transition analysis, see Supplementary Results. We determined that enhancing the helix intermediates may promote the formation of hIAPP aggregates with high ThT fluorescence intensity. However, there were no intermediates formed when hIAPP was prepared with the analog of HBS 1, UC 1, whose sequence was the same as HBS 1, but lacking a constrained conformation (Fig. S11 in SI).

To clarify the cause of the high ThT fluorescence intensity when HBS 1 was added to the system, we performed morphologic studies on these aggregation intermediates. We found that in the presence of HBS 1, hIAPP tended to assemble into large globular oligomers (Fig. 2g). The diameter was about 600 nm which corresponded to the Dynamic Light Scattering measurement (DH = 700 nm) (Fig. 2h). However, in the absence of HBS 1, hIAPP formed small oligomers with a diameter of about 80 nm (Fig. 2e). This value also corresponded with the Dynamic Light Scattering measurement (DH = 90 nm) (Fig. 2f). Both of these peptides will eventually convert to fibers (Fig. S13 in SI). We propose that the increase of ThT fluorescence intensity is caused by the large globular oligomers formed in the presence of HBS 1. The transition from these large globular aggregates to fibrils leads to the decrease of ThT fluorescence intensity and finally results in the same kinetic curve as hIAPP only.

To explain how these large oligomers formed, we investigated the formation of oligomers using enlargements of TEM images, which indicated that these large oligomers were formed by further assembly of some aggregated units (Fig. S17 in SI). By performing photo-induced cross-linking of unmodified proteins (PICUP) and sodium dodecyl sulfate polyacrylamide gel electrophoresis (SDS-PAGE) with silver staining (Fig. 2d), we found that in the presence of HBS 1, hIAPP formed large aggregated units (molecule weight is ~70kDa;) quickly. This result corresponded with a typical helix aggregation mechanism in which helix monomers will assemble into large aggregate units easily and enhance the transition to β-rich aggregates.[32] However, for hIAPP only, we only observed some small aggregate units (monomers, dimers and a few trimers). Coarse-Grain MD simulations also suggested that in the absence of HBS1, hIAPP tend to aggregate to small aggregate units (dimer and trimer). However, in the presence of HBS1, hIAPP will co-assemble with HBS 1 to large aggregate units quickly (Fig. S15, S16 in SI). Its morphology corresponded with the TEM studies. That is to say, HBS 1 promoted the formation of hIAPP large aggregate units which further assembled into large globular oligomers. It is these large

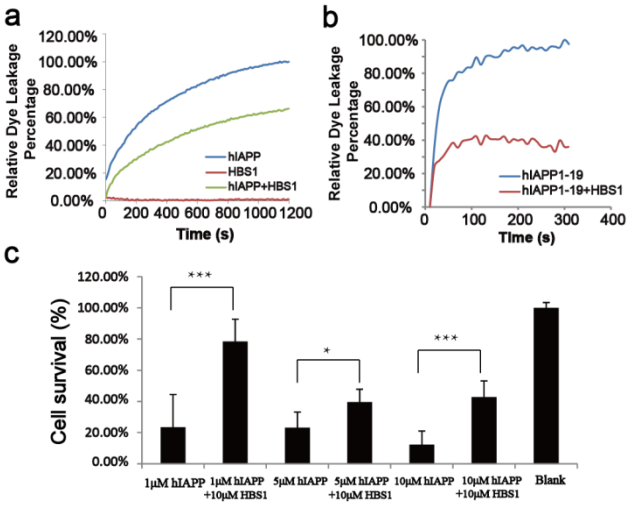

Figure 3. Effect of HBS 1 on the interaction of hIAPP and membrane. (a) Dye leakage assay from 2-oleoyl-1-palmitoyl-sn-glycero-3-phosphocholine (POPC) and 2-oleoyl-1-palmitoyl-sn-glycero-3-glycerol (POPG) (3:1) vesicles (15.68 μM) induced by full length hIAPP (hIAPP, 1 μM; blue line), hIAPP (1 μM) + HBS1 (10 μM) (green line), HBS 1 (10 μM; red line). (b) Dye leakage assay induced by hIAPP1-19 (1 μM; blue line) and hIAPP1-19 (1 μM) + HBS 1 (10 μM) (red line). (c) The viability of INS-1 rat insulinoma cells treated with hIAPP (1 μM, 5 μM, 10 μM) or hIAPP (1 μM, 5 μM, 10 μM) + HBS1 (10 μM). The level of significance indicated by ***, $p < .001$; **, $p < .01$; and *, $p < .05$ (by 2-tailed Student's t-test). The data represent the mean ±S.D. (n=4).

globular oligomers that caused the high fluorescence intensity observed in the ThT assay.

To identify whether promoting the formation of large globular oligomers will prevent cytotoxicity induced by the small hIAPP oligomers, we explored the effect of HBS 1 on the interaction between hIAPP and membrane. We found that HBS 1 decreased the relative dye leakage percentage induced by hIAPP by 40% (20% for ratio 1:1; 50% for ratio 1:100; Fig. S20 in SI.) (Fig. 3a) at 20 min and by 60% for leakage induced by hIAPP1-19 at 300 s (Fig. 3b), indicating that promoting the formation of large oligomers can indeed inhibit hIAPP toxicity. On the other hand, the unconstrained control peptide UC 1 slightly decreased the relative dye leakage percentage (Fig. S21 in SI.). Besides, from the comparison of the extended dye leakage experiment and ThT experiment, we believed that HBS 1 mainly functioned by blocking oligomer mediated membrane damage (Fig. S18, S19 in SI).

Cell viability assays established that HBS 1 can indeed reduce the toxicity of hIAPP on INS-1 cells (Fig. 3c). These assays showed that the hIAPP pre-incubated without HBS 1 killed about 70% of the INS-1 cells, relative to controls, when cells were incubated in PBS buffer solutions only. However, cell survival increased notably when cells were cultured with a pre-incubated mixture of HBS 1 and hIAPP at different concentration. Furthermore, we found that HBS 1 prevented hIAPP from changing the cell morphology from a native fusiform state to a transparent ball state. Perhaps HBS 1 blocked organelle leakage from a cell (Fig. S22 in SI.).

Conclusions

Using our understanding of the α-helix-to-β-sheet transition mechanism as a basis for our design, we synthesized a helix mimetic

regulator which promoted the formation of large nontoxic oligomers and reduced the cytotoxicity induced by small oligomers. We suggest the targeting of the helix intermediates in the very early stage of the aggregation as an alternative therapeutic approach to amyloid diseases. This study not only provided a strategy for inhibitor design based on the helix intermediates of hIAPP but also revealed some clues toward understanding the molecular events involved in hIAPP aggregation.

This work was supported by the major State Basic Research Development Program of China (973 program) (No. 2013CB910700, 2012CB821600) and grants from the National Natural Science Foundation of China (No. 91313301, 21472109, 021261130090). This work was supported by Tsinghua National Laboratory for Information Science and Technology and Beijing Nuclear Magnetic Resonance Center. We thank Prof. Zhixiang Yu in Peking University for help with the microwave synthesis, Hong Liu, Dongxiang Liu, Yechun Xu in Shanghai Institute of Materia Medica Chinese Academy of Sciences and Dong Wang in Tsinghua University for helpful comments on molecule dynamics simulation.

Notes and references

[a] Department of Chemistry, Key Laboratory of Bioorganic Phosphorus Chemistry & Chemical Biology (Ministry of Education), Tsinghua University, Beijing 10084, P. R. China. Fax: (+86)10-62781695. E-mail: liym@mail.tsinghua.edu.cn

[b] Beijing Institute for Brain Disorders Center of Parkinson's Disease

Electronic Supplementary Information (ESI) available: Supplementary materials, methods, results, and references. See DOI: 10.1039/c000000x/

1 G. J. Cooper, *Endocr. Rev.*, 1994, **15**, 163-201.
2 P. Westermark, C. Wernstedt, E. Wilander, D. W. Hayden, T. D. O'Brien and K. H. Johnson, *Proc. Natl. Acad. Sci. U. S. A.*, 1987, **84**, 3881-3885.
3 A. Kapurniotu, A. Schmauder and K. Tenidis, *J. Mol. Biol.*, 2002, **315**, 339-350.
4 S. Gilead and E. Gazit, *Angew. Chem. Int. Ed. Engl.*, 2004, **43**, 4041-4044.
5 R. Mishra, B. Bulic, D. Sellin, S. Jha, H. Waldmann and R. Winter, *Angew. Chem. Int. Ed. Engl.*, 2008, **47**, 4679-4682.
6 R. Mishra, D. Sellin, D. Radovan, A. Gohlke and R. Winter, *Chembiochem*, 2009, **10**, 445-449.
7 J. Zheng, C. Liu, M. R. Sawaya, B. Vadla, S. Khan, R. J. Woods, D. Eisenberg, W. J. Goux and J. S. Nowick, *J. Am. Chem. Soc.*, 2011, **133**, 3144-3157.
8 A. Mishra, A. Misra, T. S. Vaishnavi, C. Thota, M. Gupta, S. Ramakumar and V. S. Chauhan, *Chem. Commun. (Camb)*, 2013, **49**, 2688-2690.
9 L. M. Yan, M. Tatarek-Nossol, A. Velkova, A. Kazantzis and A. Kapurniotu, *Proc. Natl. Acad. Sci. U. S. A.*, 2006, **103**, 2046-2051.
10 J. Hu, Y. P. Yu, W. Cui, C. L. Fang, W. H. Wu, Y. F. Zhao and Y. M. Li, *Chem. Commun. (Camb)*, 2010, **46**, 8023-8025.
11 G. J. S. Cooper, J. F. Aitken and S. Zhang, *Diabetologia*, 2010, **53**, 1011-1016.
12 J. R. Brender, S. Salamekh and A. Ramamoorthy, *Acc. Chem. Res.*, 2012, **45**, 454-462.
13 R. A. Ritzel, J. J. Meier, C. Y. Lin, J. D. Veldhuis and P. C. Butler, *Diabetes*, 2007, **56**, 65-71.
14 Y. P. Yu, P. Lei, J. Hu, W. H. Wu, Y. F. Zhao and Y. M. Li, *Chem. Commun. (Camb)*, 2010, **46**, 6909-6911.
15 M. S. Chen, D. S. Zhao, Y. P. Yu, W. W. Li, Y. X. Chen, Y. F. Zhao and Y. M. Li, *Chem. Commun. (Camb)*, 2013, **49**, 1799-1801.
16 I. Saraogi, J. A. Hebda, J. Becerril, L. A. Estroff, A. D. Miranker and A. D. Hamilton, *Angew. Chem. Int. Ed. Engl*, 2010, **49**, 736-739.
17 Y. Xu, J. Shen, X. Luo, W. Zhu, K. Chen, J. Ma and H. Jiang, *Proc. Natl. Acad. Sci. U. S. A.*, 2005, **102**, 5403-5407.
18 D. Liu, Y. Xu, Y. Feng, H. Liu, X. Shen, K. Chen, J. Ma and H. Jiang, *Biochemistry*, 2006, **45**, 10963-10972.
19 Y. Hong, L. Meng, S. Chen, C. W. Leung, L. T. Da, M. Faisal, D. A. Silva, J. Liu, J. W. Lam, X. Huang and B. Z. Tang, *J. Am. Chem. Soc.*, 2012, **134**, 1680-1689.
20 A. Laganowsky, C. Liu, M. R. Sawaya, J. P. Whitelegge, J. Park, M. Zhao, A. Pensalfini, A. B. Soriaga, M. Landau, P. K. Teng, D. Cascio, C. Glabe and D. Eisenberg, *Science*, 2012, **335**, 1228-1231.
21 J. C. Stroud, C. Liu, P. K. Teng and D. Eisenberg, *Proc. Natl. Acad. Sci. U. S. A.*, 2012, **109**, 7717-7722.
22 N. F. Dupuis, C. Wu, J.-E. Shea and M. T. Bowers, *J. Am. Chem. Soc.*, 2011, **133**, 7240-7243.
23 N. F. Dupuis, C. Wu, J. E. Shea and M. T. Bowers, *J. Am. Chem. Soc.*, 2009, **131**, 18283-18292.
24 J. J. Wiltzius, S. A. Sievers, M. R. Sawaya and D. Eisenberg, *Protein Sci.*, 2009, **18**, 1521-1530.
25 L. K. Henchey, J. R. Porter, I. Ghosh and P. S. Arora, *Chembiochem*, 2010, **11**, 2104-2107.
26 L. K. Henchey, S. Kushal, R. Dubey, R. N. Chapman, B. Z. Olenyuk and P. S. Arora, *J. Am. Chem. Soc.*, 2010, **132**, 941-943.
27 E. L. Humphris and T. Kortemme, *Structure*, 2008, **16**, 1777-1788.
28 R. N. Chapman and P. S. Arora, *Org. Lett.*, 2006, **8**, 5825-5828.
29 R. N. Chapman, G. Dimartino and P. S. Arora, *J. Am. Chem. Soc.*, 2004, **126**, 12252-12253.
30 D. Wang, K. Chen, J. L. Kulp Iii and P. S. Arora, *J. Am. Chem. Soc.*, 2006, **128**, 9248-9256.
31 Y. Fezoui and D. B. Teplow, *J. Biol. Chem.*, 2002, **277**, 36948-36954.
32 A. Abedini and D. P. Raleigh, *Phys. Biol.*, 2009, **6**, 015005.